SUPPLEMENTAL DATA

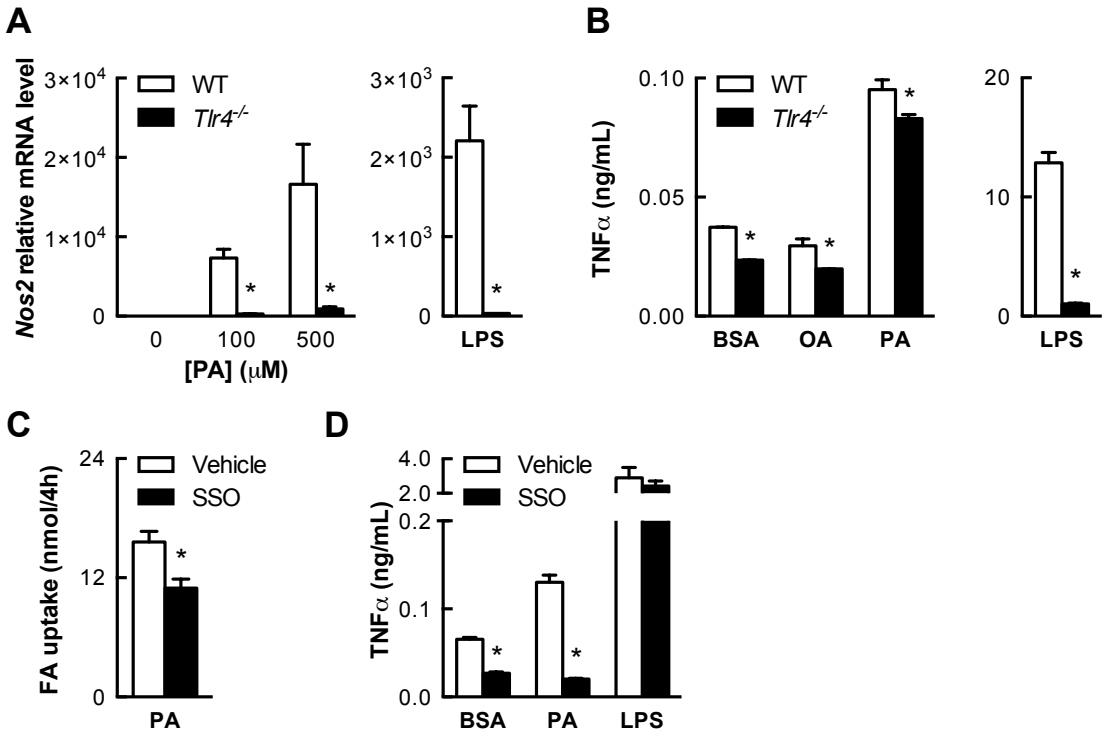

Figure S1 (Related to Figure 1). SFAs and LPS induce inflammatory activation through distinct mechanisms

(A) The M_{LPS} inflammatory marker *Nos2*, measured by quantitative PCR, is up-regulated by treatment with PA (12 h) and LPS (100 ng/mL, 16 h) in wild type BMDCs but not in *Tlr4*$^{-/-}$ BMDCs (n=2-3). (B) TNF secretion stimulated by PA (500 μM, 24 h) is largely intact in *Tlr4*$^{-/-}$ BMDCs, whereas LPS-induced TNF secretion is substantially abrogated by TLR4 deficiency (n=3). (C) Inhibition of ^{14}C PA uptake by sulfo-n-succinimidyl oleate (SSO, 500 μM, n=6). (D) Abrogation of PA (500 μM)- but not LPS (200 ng/mL)-stimulated TNF secretion by SSO co-treatment (24 h, n=3-4). Error bars, SD. *, $p<0.05$ vs. WT (A,B) or vehicle (C,D).

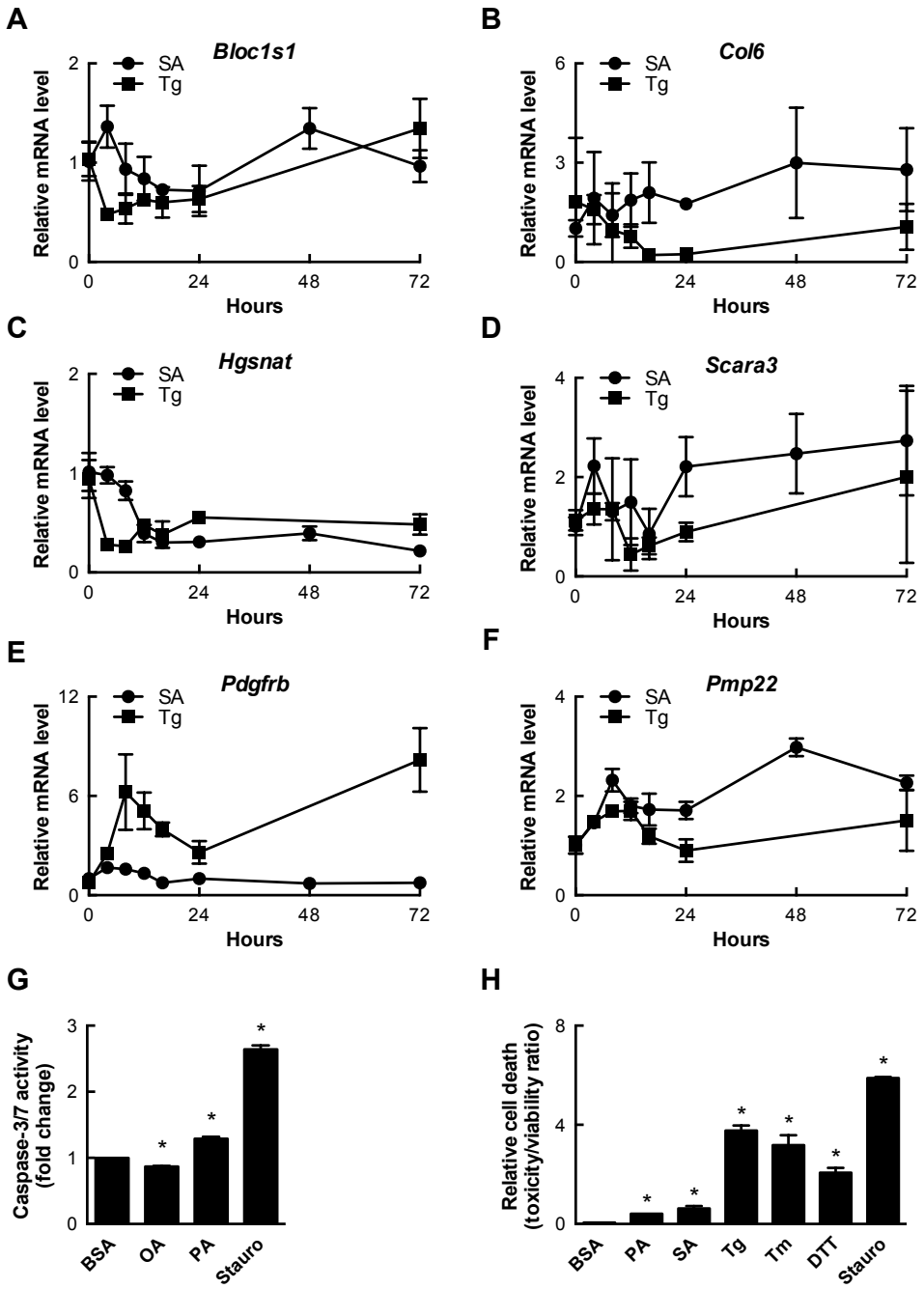

Figure S2 (Related to Figure 2). SFAs do not induce widespread RIDD activation or cell death in BMDCs.

(A-F) mRNA levels of RIDD markers in BMDCs (n=2-3) treated with SA (500 μM) or thapsigargin (200 nM). (G) Caspase-3/7 activity in BMDCs (n=2) treated with FAs (500 μM, 24 h) or staurosporine (1 μM, 6 h, positive control). (H) Ratio of dead-to-live cell protease activity (measured using fluorescent substrates, n=4) in BMDCs treated with SFAs or staurosporine as in (G) or classical ER stress inducers (200 nM Tg, 5 μg/mL Tm, 2.5 mM DTT, 24 h). Data in (H) also appear as vehicle condition in Figure 7C. Error bars, SD. *, $p<0.05$ vs. BSA (G, H).

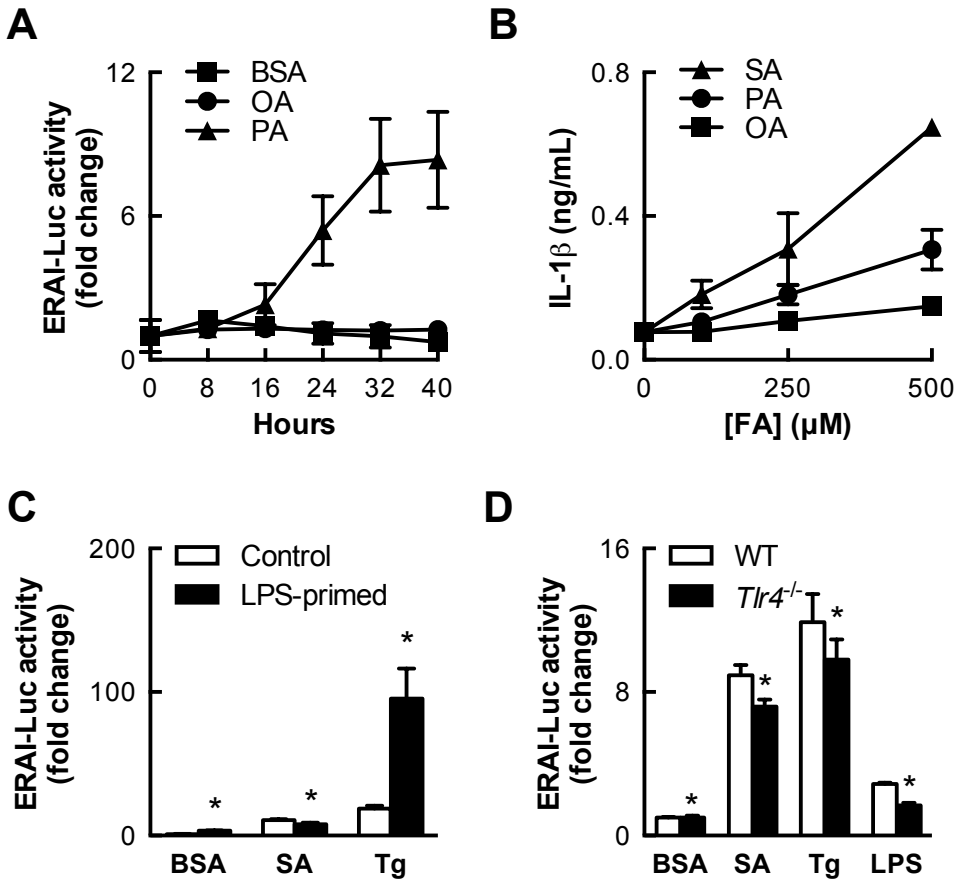

Figure S3 (Related to Figure 4). Responses to SFAs and LPS in BMDMs and BMDCs

(A) Time course of IRE1α reporter activity in BMDMs treated with FAs (500 μM, n=3-4). (B) IL-1β secretion by LPS-primed BMDMs treated FAs (24 h, n=3). (C) IRE1α reporter activity in BMDCs (n=3-5) treated for 24 h with SA (500 μM) or Tg (200 nM) with or without LPS priming (3 h, 200 ng/mL). (D) IRE1α reporter activity in *Tlr4*$^{-/-}$ BMDCs, showing that the response to LPS treatment is reduced to a greater extent than that to SA treatment (500 μM, 24 h, n=4-6). Error bars, SD. *, $p<0.05$ vs. control (C) or WT (D).

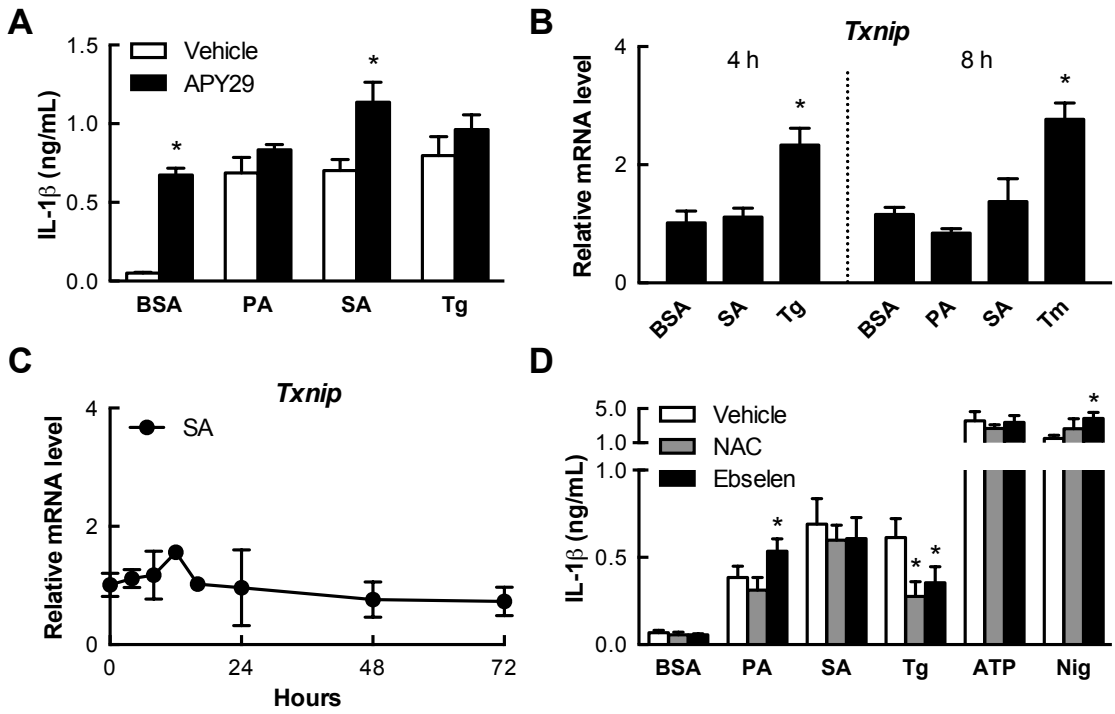

Figure S4 (Related to Figure 5). SFA-induced NLRP3 inflammasome activation does not involve TXNIP induction or ROS

(A) IL-1β secretion by BMDCs co-treated with APY29 (1 μM), showing that IRE1α kinase inhibition and endoribonuclease activation induces IL-1β secretion on its own and does not diminish that induced by SFAs (500 μM, 24 h, n=4). (B) Increased mRNA levels of the terminal UPR marker *Txnip*, measured with quantitative PCR, by treatment with thapsigargin (200 nM) and tunicamycin (5 μg/mL) but not SFAs (500 μM) in BMDCs (n=3-4). (C) Prolonged SA treatment (500 μM) does not increase *Txnip* mRNA levels in BMDCs (n=2-3). (D) IL-1β secretion by BMDCs co-treated with the antioxidants N-acetylcysteine (NAC) and ebselen, showing that antioxidants reduce IL-1β secretion stimulated by Tg but not SFAs (n=4). Error bars, SD. *, $p<0.05$ vs. vehicle (A,D) or BSA (B).

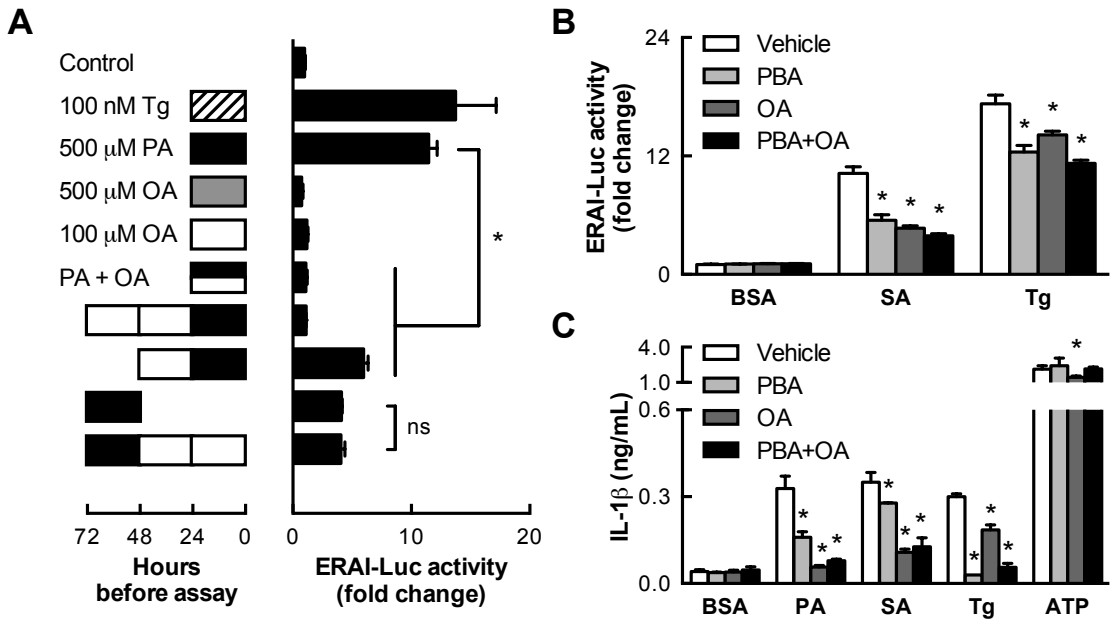

Figure S5 (Related to Figure 6). Combination of PBA and OA does not diminish SFA-induced IRE1α or NLRP3 inflammasome activation more than PBA or OA alone

(A) Abrogation of PA-induced IRE1α reporter activity by co-treatment or pretreatment with OA (100 μM) but not by OA treatment following PA exposure in BMDCs (n=3). (B,C) OA (100 μM) and the chemical chaperone PBA (1 mM) both reduce IRE1α reporter activity (B, n=5-6) and IL-1β secretion (C, n=4) induced by SFAs (500 μM) or Tg (200 nM) but have no additive effect in combination. Similar findings were obtained using TUDCA (data not shown). (C) Error bars, SD. *, $p<0.05$ vs. vehicle (B, C) or as indicated.

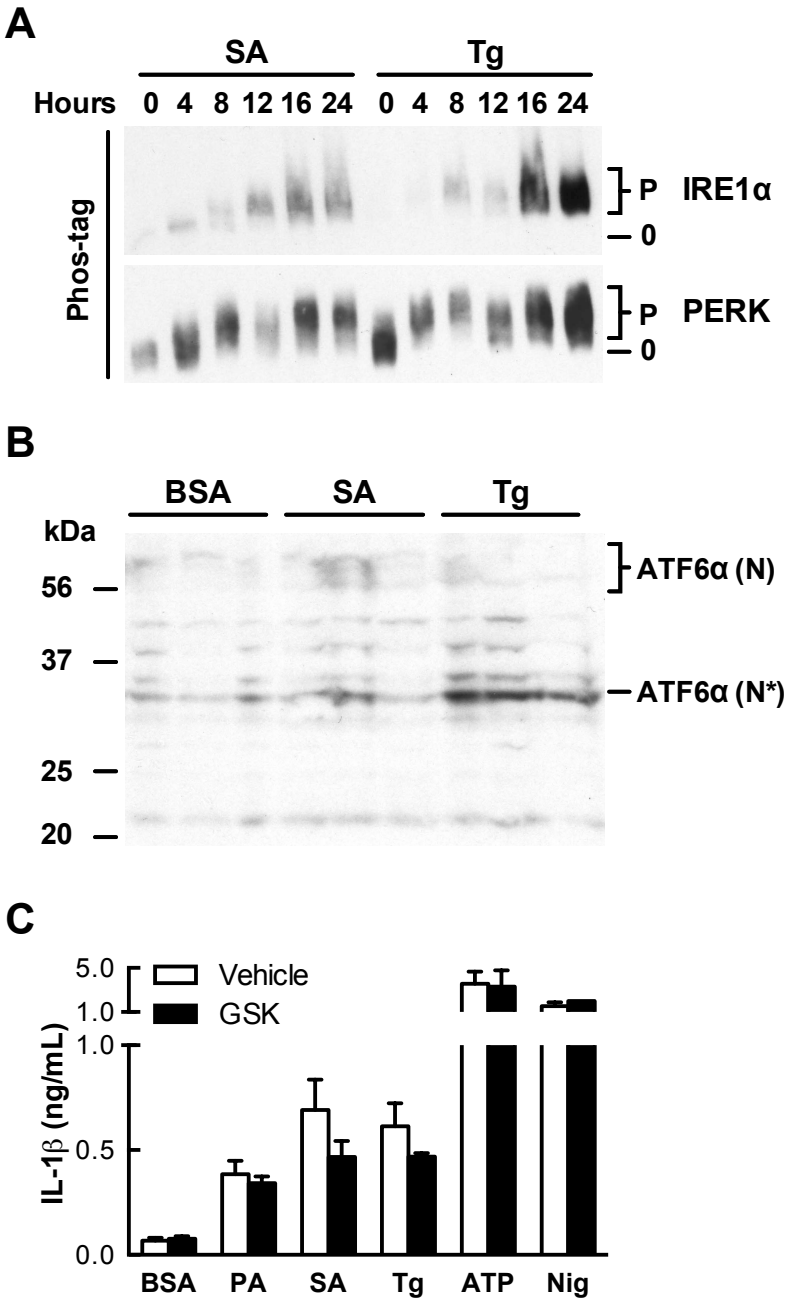

Figure S6 (Related to Figure 6). SA treatment robustly activates IRE1α and PERK but not ATF6α

(A) Phosphorylation of IRE1α and PERK, detected by slower migration through Phos-tag agarose, induced by SA (500 μM) and Tg (200 nM) in BMDCs. (B) Enrichment of cleaved ATF6α in nuclear fractions of BMDCs treated for 20 h with Tg but not SA. We detect primarily a ~33 kDa nuclear fragment of ATF6α (N*); similarly sized fragments have been previously reported and are likely degradation products of the active nuclear form of ATF6α (N, Thuerauf et al., 2002). (C) IL-1β secretion induced by SFAs (500 μM, 24 h, n=3-4) is not diminished by co-treatment with PERK inhibitor GSK 2656157 (500 nM). Error bars, SD.

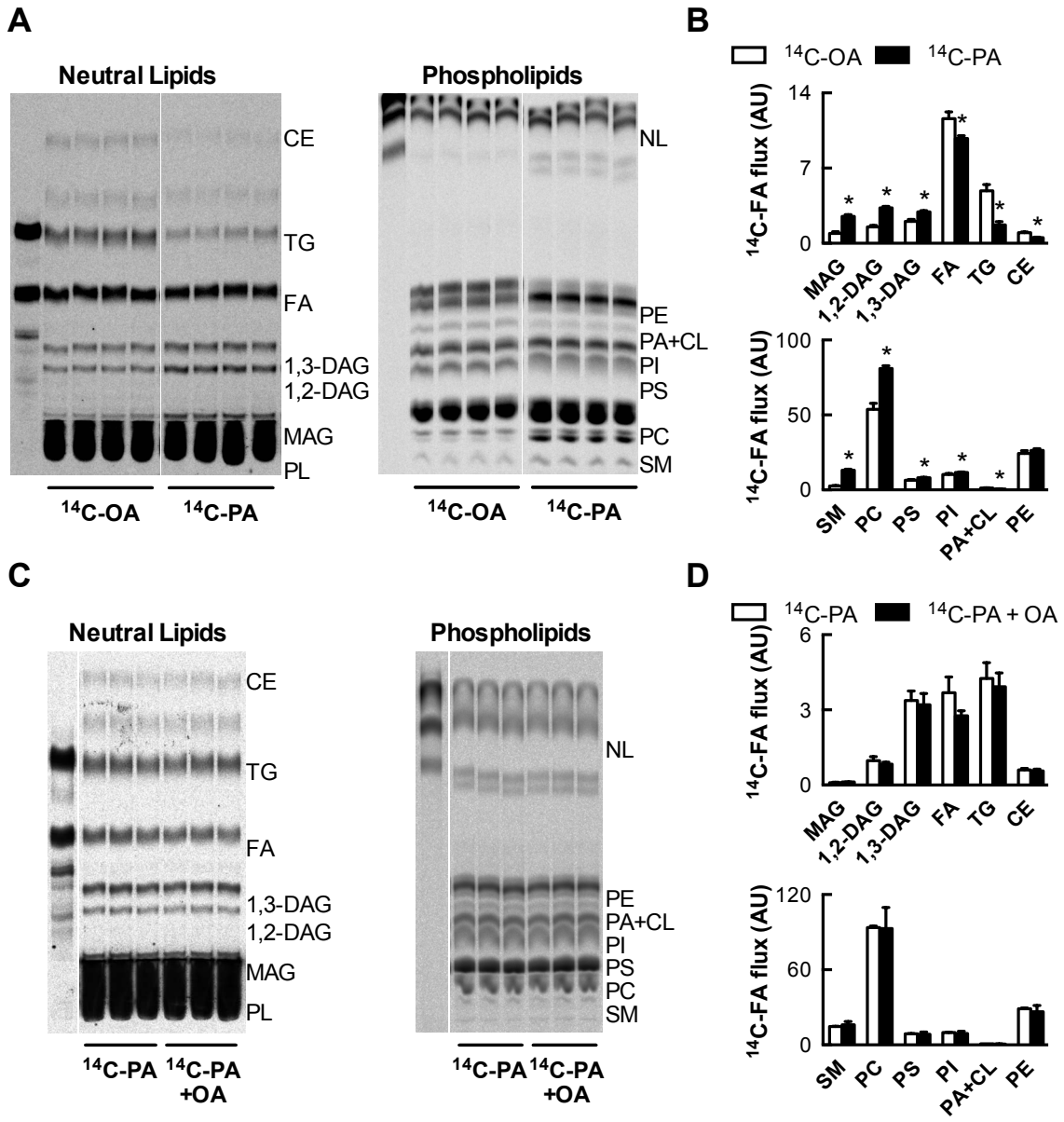

Figure S7 (Related to Figure 6). OA and PA flux to distinct lipid compartments, and OA co-treatment does not modulate the pattern of PA flux

(A) Differential flux of radiolabeled OA and PA into neutral lipid and phospholipid species as determined by TLC and autoradiography. PL, phospholipids; MAG, monoacylglycerol; DAG, diacylglycerol; TG, triacylglycerol, FA, fatty acid; CE, cholesterol ester; SM, sphingomyelin; PC, phosphatidylcholine; PS, phosphatidylserine; PI, phosphatidylinositol; PA+CL, phosphatidic acid and cardiolipin (bands indistinguishable); PE, phosphatidylethanolamine; NL, neutral lipids. ^{14}C-OA and ^{14}C-PA images were taken from separate sections of the same TLC plate (n=4). (B) Quantification of (A). AU, arbitrary units. (C) Lack of change in the flux of radiolabeled PA, measured as in (A), by co-treatment with unlabeled OA (n=3). (D) Quantification of (C). Error bars, SD. *, $p<0.05$ vs. ^{14}C-OA (B) or ^{14}C-PA (D).

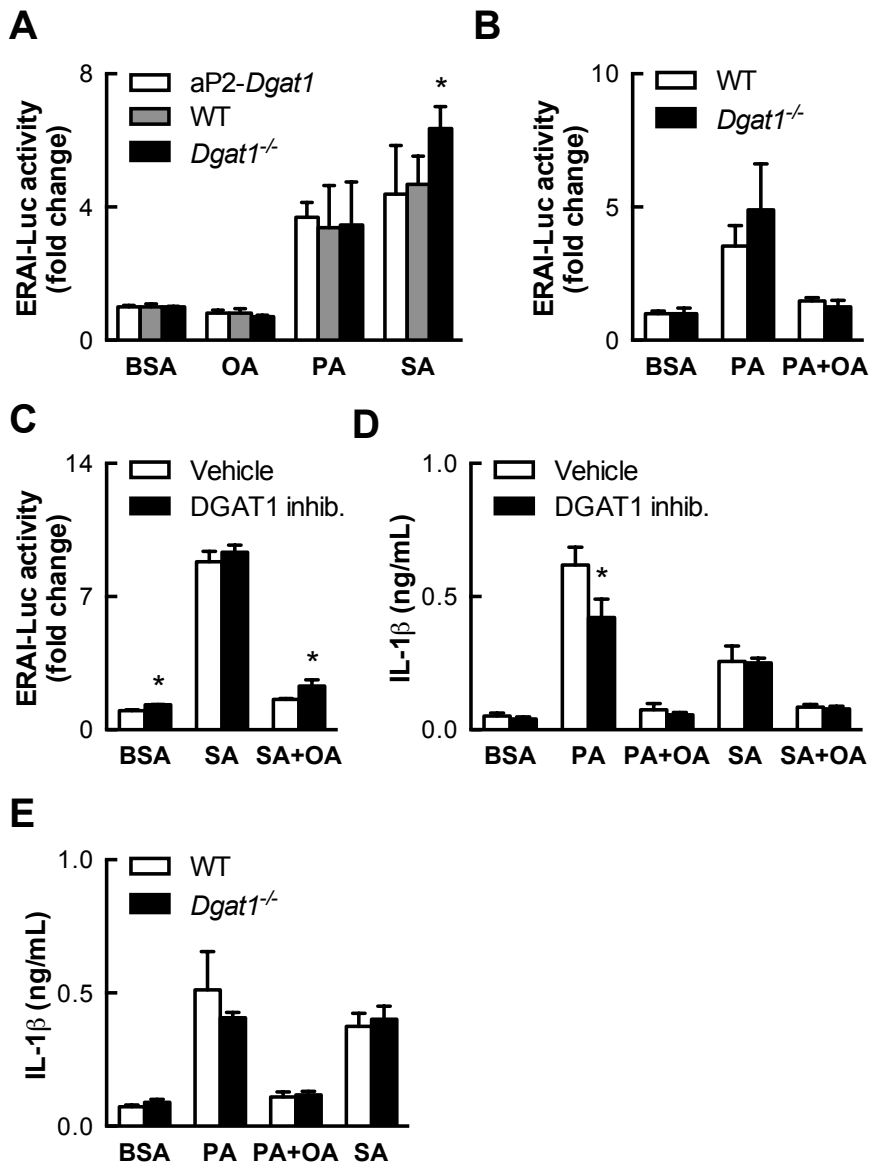

Figure S8 (Related to Figure 6). DGAT1 activity does not control SFA-induced IRE1α or NLRP3 inflammasome activation

(A) IRE1α reporter activity, showing that the response to SFAs (400 μM, 24 h) is largely unchanged in BMDCs lacking (*Dgat1*$^{-/-}$) or overexpressing (*aP2-Dgat1*) the triacylglycerol synthesis enzyme DGAT1. (B) IRE1α reporter activity in *Dgat1*$^{-/-}$ BMDCs, showing retention of the ability of OA co-treatment (100 μM) to abrogate reporter activity induced by PA (600 μM, 24 h). (C) Inhibition of DGAT1 does not affect IRE1α reporter activation by SA (500 μM, 24 h) or the protective effect of OA co-treatment (100 μM). (D) IL-1β secretion by BMDCs, showing that DGAT1 inhibition modestly reduces IL-1β secretion induced by PA but not SA (500 μM, 24 h) and does not affect protection by OA co-treatment (100 μM). (E) IL-1β secretion in response to SFAs (500 μM, 24 h) and the impact of OA co-treatment (100 μM) are unaltered in *Dgat1*$^{-/-}$ BMDCs. n=4 for all treatments. Error bars, SD. *, $p<0.05$ vs. WT (A,B,E) or vehicle (C,D).

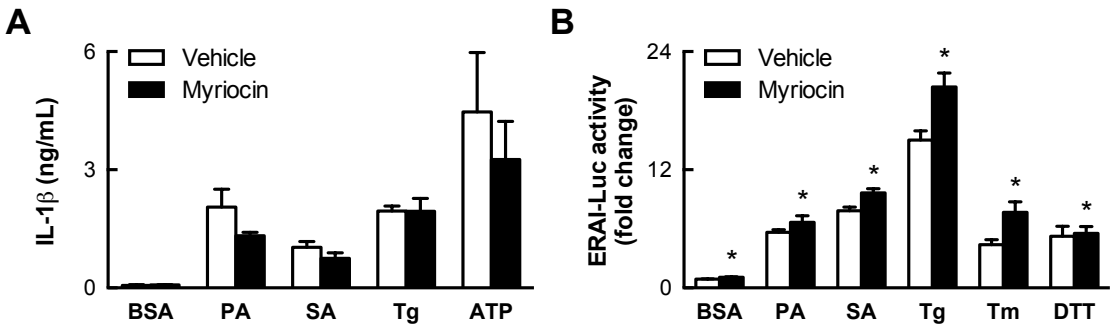

Figure S9 (Related to Figure 7). Limiting the flux of SFAs into sphingolipids does not reduce SFA-induced IRE1α or NLRP3 inflammasome activation

(A) IL-1β secretion by BMDCs, showing a modest trend toward reduction of SFA (500 μM, 24 h)-induced, but not Tg or ATP-induced IL-1β secretion by the sphingolipid biosynthesis inhibitor myriocin (n=4). (B) Lack of impact of myriocin on the ability of SFAs (1 mM PA, 500 μM SA, 24 h) or classical ER stress inducers to stimulate IRE1α reporter activity (n=6). Error bars, SD. *, $p<0.05$ vs. vehicle.

Table S1 (Related to Figure 1). Differentially expressed genes in BMDMs treated with SA, OA, or LPS

Lists of differentially expressed genes for each treatment are provided in a separate Excel spreadsheet.

SUPPLEMENTAL EXPERIMENTAL PROCEDURES

SVF isolation: Visceral adipose tissue (epididymal, perirenal, and mesenteric fat pads) was collected from PBS-perfused 16-24 week old male C57Bl6 mice after consumption of chow or HFD (Harlan Teklad TD.88137) for 12 weeks. Approximately 1 g of pooled VAT was digested for 1 h in a 37 °C shaking incubator with 0.66 mg/mL Type I Collagenase (Worthington) in Krebs Ringer Buffer with 1% BSA, filtered through a 100 μm cell strainer, and centrifuged at 200 x g from 10 minutes to separate the SVF from the adipocytes. SVF pellets were incubated in ACK buffer for 5 minutes to lyse the erythrocytes and resuspended in TRIzol reagents (Life Technologies) for RNA isolation.

Isolation of primary bone marrow-derived MCs: Bone marrow was flushed and pooled from the femurs and tibias of mice (6-12 week old, mixed gender), triturated in RPMI 1640 (Gibco), filtered through a 70 μm cell strainer, and incubated in ACK buffer for 5 minutes. Bone marrow cells were plated in non-tissue culture treated multi-well plates at a density of 2000 cells/mm^2 and cultured in RPMI supplemented with 10% FBS (Atlanta Biologicals), penicillin/streptomycin, and 10 ng/mL of either recombinant GM-CSF (for BMDCs; Peprotech) or recombinant M-CSF (for BMDMs; Peprotech). Media was replenished on day 3 and replaced on day 6. Growth factors were removed from the media after 6-8 days of differentiation, and adherent cells were used for experiments 1-10 days later.

FA preparation: FAs (Nu-Chek Prep) were dissolved in 70 °C water, and 1 M NaOH was added drop-wise to yield a clear solution (Listenberger, 2001). The resulting aqueous FA

preparations (20 mM) were complexed at a 2:1 FA:BSA molar ratio with 20% FA-free, low-endotoxin BSA (Sigma Aldrich A8806) heated to 37 °C. FA stock concentrations were measured using a colorimetric NEFA assay kit (Wako), and aliquots were stored at -20 °C. FA stocks prepared this way had very low levels of endotoxin contamination according to colorimetric LAL assays (Lonza).

Liposome preparation: DOPC liposomes were supplemented with 10% dioleoylphosphatidylserine (DOPS) to both enhance cellular uptake of the liposomes and aid in the formation of small unilamellar vesicles, which do not always form readily from preparations of 100% PC. To accomplish this, chloroform stocks of DOPC and DOPS (Avanti Polar Lipids) were combined at a 10:1 molar ratio of DOPC:DOPS (2 μg total), dried down under a stream of nitrogen, lyophilized for 3 hours, and rehydrated with 1 mL PBS in a 65 °C shaker for 1 hour. Liposome preparations were then sonicated in a 65 °C water bath until they turned clear (2-3 hours) and stored at 4 °C. Prior to addition to media, liposome preparations were heated to 65 °C and sonicated for 10-15 minutes.

FA uptake: BMDCs were pre-treated with 500 μM SSO (Toronto Research Chemicals) in DMSO or DMSO alone for 45 minutes prior to co-treatment with 500 μM PA containing 0.5 μCi/mL ^{14}C-PA (Moravek Biochemicals) for 4 hours. Media was then removed and cells were washed three times with Krebs Ringer Buffer containing 0.5% BSA and 500 μM phloretin (Santa Cruz Biotechnology) and lysed with 1 M NaOH. Lysate radioactivity was measured by liquid scintillation counting.

FA flux: BMDCs were treated for 16 hours with 100 μM PA or OA containing 0.1 μCi/mL ^{14}C-PA or ^{14}C-OA (Moravek Biochemicals), respectively. Unlabeled OA (20 μM) was added to cells treated with radiolabeled PA in order to determine the impact of OA co-treatment on intracellular PA flux. After incubation, cells were washed three times with PBS and cellular lipids were extracted using 2:1 chloroform:methanol (Bligh and Dyer, 1959). Lipids in the lower organic phase were dried down under a stream of nitrogen, resuspended in chloroform, spotted on silica plates (Whatman), and resolved by thin layer chromatography using either hexane:ethyl ether:acetic acid (80:20:2) to separate neutral lipids or methyl acetate: isopropanol:chloroform:methanol:0.25% aqueous KCl (25:25:25:10:9) to separate phospholipids (Vitiello and Zanetta, 1978). Air-dried TLC plates were exposed to iodine vapor to visualize bands, and reference standards were used to identify lipid species. Radioactivity was then detected with a Fuji Scanner FLA-5100 phosphorimager and quantified using Multigauge software (Fujifilm).

Real-time quantitative PCR: RNA was isolated using TRIzol reagent (Life Technologies), and 0.2-1 μg total RNA was reverse-transcribed using the Superscript III Reverse Transcriptase (Life Technologies) and random hexamers according to the manufacturer's instructions. Quantitative RT-PCR was performed on an ABI Prism 7900HT using Power SYBR Green master mix (Life Technologies). Relative expression differences were calculated using the ΔΔCT method and either *Hprt* or *Ppib* as a reference gene.

Primers used for RT-PCR

Primer	Sequence
Dnajc3 F	GTGGCATCCAGATAATTTCCAG
Dnajc3 R	GAGTTCCAACTTCTGTGGAAGG
Erdj4 F	CTTAGGTGTGCCAAAGTCTGC
Erdj4 R	GGCATCCGAGAGTGTTTCATA
Ern1 F	CCTGCAACCTTGACTGTTTCC
Ern1 R	TCTATTCGGTCACTTACATCCTG
Ero1l F	CGGACCAAGTTATGAGTTCCA
Ero1l R	TCAGAGAGATTCTGCCCTTCA
Hprt F	TCAGTCAACGGGGGACATAAA
Hprt R	GGGGCTGTACTGCTTAACCAG
Il1b F	GCAACTGTTCCTGAACTCAACT
Il1b F	ATCTTTTGGGGTCCGTCAACT
Nlrp3 F	ATTACCCGCCCGAGAAAGG
Nlrp3 R	TCGCAGCAAAGATCCACACAG
Nos2 F	CCAAGCCCTCACCTACTTCC
Nos2 R	CTCTGAGGGCTGACACAAGG
Ppib F	TGGAAGAGCACCAAGACAGAC
Ppib R	TGCCGGAGTCGACAATGAT
Pycard F	CTTGTCAGGGGATGAACTCAAA
Pycard R	GCCATACGACTCCAGATAGTAG
Txnip F	TCAAGGGCCCCTGGGAACATC
Txnip R	GACACTGGTGCCATTAAGTAG
Xbp1^{t} F	GACAGAGAGTCAAACTAACGT
Xbp1^{t} R	GTCCAGCAGGCAAGAAGGT
Xbp1^{s} F	AGCTTTTACGGGAGAAAACTCA
Xbp1^{s} R	GCCTGCACCTGCTGCG

Luciferase assays: ERAI-Luc BMDCs were seeded onto 96-well plates (7 x 10^4 cells/well) one day prior to FA treatment. In experiments using pharmacological inhibitors, cells were pretreated with inhibitor alone for 1-3 hours before addition of FAs or other stimuli. After treatment, cells were lysed and luciferase activity was measured well-by-well following injection of luciferin (Gold Biotechnology) using a Mithras luminometer (Berthold) as described (Tomlinson et al., 2004). Luciferase activities are expressed as fold changes compared to untreated or vehicle-treated cells within the same plate.

Cell death assays: Caspase-3/7 activity was measured by the EnzChek Caspase-3 Assay Kit (Molecular Probes). Overall cell death was assessed by the ratio of dead cell protease activity to live cell protease activity using fluorogenic substrates from the ApoTox Glo kit (Promega).

Immunoblotting and immunofluorescence: IRE1α and PERK phosphorylation was assessed in whole cell lysates (in RIPA buffer with protease and phosphatase inhibitors [Santa Cruz Biotechnology]) using Phos-tag gels as described (Qi et al., 2011). For measurement of ATF6α, nuclear fractions were obtained by centrifugation. Briefly, cells were detached with trypsin, resuspended in cellular lysis buffer (150 mM NaCl, 20 mM Tris-HCl [pH 7.4], 0.5% Triton X-100, 1 mM PMSF, 100 μM sodium orthovanadate, 1x protease inhibitor cocktail [Santa Cruz Biotechnology]), and spun at 800 x g for 2 minutes. Pelleted nuclei were then resuspended in nuclear lysis buffer (420 mM NaCl, 20 mM Tris-HCl [pH 8.0], 1.5 mM MgCls, 0.2 mM EDTA, 25% glycerol; Beg et al., 1993), incubated on ice for 30 minutes, and centrifuged at 16,000 x g for 10 minutes. The resulting supernatants were loaded onto 10% SDS-PAGE and transferred onto PVDF membranes (Bio-Rad). Membranes were blocked overnight (4ºC) in 0.1% Tween-20 containing 5% BSA (TBS-T), and after washing, were incubated in TBS-T containing primary antibodies. Membranes were then washed and incubated in TBS-T containing 1:5000 HRP-conjugated anti-rabbit IgG (ECL, GE Healthcare). Immunoreactive bands were detected by chemiluminiscence (Super Signal West Pico, Thermo Scientific). For imaging of ASC puncta, BMDCs were replated onto glass coverslips one day prior to stimulation and fixed with 4% PFA in PBS containing 3% sucrose for 10 minutes. Cells were then permeabilized with 0.1% Triton X-100 for 2 minutes, washed with PBS, and blocked with 0.2% BSA, 100mM glycine, and 10%

goat serum in PBS for 30 minutes. ASC antibody (1:200 dilution) was incubated for 1 hour followed by a goat anti-rabbit-AF 488 at 1:500. Nuclear staining was performed using DAPI (1 mg/ml) in PBS for 5 minutes. Cells were then mounted with an antifade solution (Vectashield). Images were acquired using the Zeiss Axio Imager 2 apotome upright widefield microscope. Antibodies against IRE1α (14C10) and PERK (C33E10) were purchased from Cell Signaling; ATF6α (H-280) and ASC (N-15) antibodies were from Santa Cruz Biotechnology.

SUPPLEMENTAL REFERENCES

Beg, A.A., Finco, T.S., Nantermet, P.V., and Baldwin, A.S. (1993). Tumor necrosis factor and interleukin-1 lead to phosphorylation and loss of I kappa B alpha: a mechanism for NF-kappa B activation. Mol. Cell. Biol. *13*, 3301–3310.

Bligh, E.G., and Dyer, W.J. (1959). A rapid method of total lipid extraction and purification. Can J Biochem Physiol *37*, 911–917.

Listenberger, L.L., Ory, D.S., and Schaffer, J.E. (2001). Palmitate-induced Apoptosis Can Occur through a Ceramide-independent Pathway. J. Biol. Chem. *276*, 14890–14895.

Qi, L., Yang, L., and Chen, H. (2011). Detecting and quantitating physiological endoplasmic reticulum stress. Meth. Enzymol. *490*, 137–146.

Thuerauf, D.J., Morrison, L.E., Hoover, H., and Glembotski, C.C. (2002). Coordination of ATF6-mediated transcription and ATF6 degradation by a domain that is shared with the viral transcription factor, VP16. J. Biol. Chem. *277*, 20734–20739.

Tomlinson, M.G., Kane, L.P., Su, J., Kadlecek, T.A., Mollenauer, M.N., and Weiss, A. (2004). Expression and function of Tec, Itk, and Btk in lymphocytes: evidence for a unique role for Tec. Mol. Cell. Biol. *24*, 2455–2466.

Vitiello, F., and Zanetta, J.P. (1978). Thin-layer chromatography of phospholipids. J. Chromatogr. *166*, 637–640.